JOURNAL OF MATERIALS SCIENCE 28 (1993) 1007–1014

Sintering and crystallization of a glass powder in the $MgO–Al_2O_3–SiO_2–ZrO_2$ system

M. I. BUDD
GEC ALSTHOM Engineering Research Centre, Stafford ST17 4LN, UK

The sintering and crystallization behaviour was studied of a glass powder in the $MgO–Al_2O_3–SiO_2–ZrO_2$ system in which the main crystal phases to form are clino-enstatite ($MgSiO_3$) and cubic zirconia (c–ZrO_2). During isothermal, atmospheric sintering of the glass powder, a fine dispersion of c–ZrO_2 particles, 50–100 nm diameter, was observed to form, but this did not appear to inhibit the sintering process. Nucleation of the main crystal phase, clino-enstatite, occurred both within the original glass powder particles and at the former particle surfaces, but the rate of crystallization was greater at the former particle surfaces. The c–ZrO_2 precipitates are thought to act as nucleation sites for the crystallization of the clino-enstatite. Relative densities of up to 98% were attainable during sintering, and were reached at a stage where a significant degree of crystal phase development had already taken place, proving that completion of sintering prior to the commencement of crystallization is not always a pre-requisite for the attainment of high final densities. In the material studied, the large volume contraction ($\sim$ 11%) on crystallization and the possible release of dissolved gases led to a decrease in relative density as crystallization proceeded. The relative density after complete crystallization was found to be 94% $\pm$ 1%, irrespective of the temperature and duration of the initial sintering stage of heat-treatment, and it appeared that most of the residual porosity was a result of the volume contraction on crystallization rather than poor densification during sintering.

1. Introduction

There are many applications in which glass-ceramic-based materials are advantageously produced via the sintering and controlled devitrification of glass powders, for instance, in the production of cordierite-based substrates for micro-electronic circuitry via tape casting [1, 2], the fabrication of ceramic heat-exchangers [3], and the preparation of ceramic matrix composites [4–7]. In all of these cases it is essential that the final glass-ceramic material should have low porosity and good strength, so it is important to understand the precise mechanisms by which the starting powders are transformed from an assemblage of amorphous particles into a dense and strongly bonded mass of microcrystalline phases during the heat-treatment process.

During the heat-treatment of such powders there is competition between the processes of sintering and crystallization, and it is generally considered that a high final density can only be achieved if sintering proceeds almost to completion before the precipitation of crystalline phases commences and causes the viscosity of the material to increase to such an extent that continued densification via viscous flow becomes impossible [8–10]. It has been suggested that glass-ceramics which exhibit efficient bulk nucleation are unsuitable for processing via a powder route because, on heat-treatment, they rapidly develop crystalline phases which inhibit further sintering [3].

It has been further proposed that glasses in which the nucleation of crystal phases is predominantly heterogeneous (i.e. surface rather than bulk nucleated) are more suitable for powder processing because the overall rate of crystallization is much lower than in materials exhibiting efficient homogeneous nucleation. Thus, by delaying the crystallization process, the chances of sintering to high density are enhanced. If the rate of surface-nucleated crystallization is too high, however, great difficulties are still encountered in sintering, and high relative densities cannot be reached [8]. This problem may arise if the glass powders are too fine.

In the present study, the sintering and crystallization behaviour of a glass in the $MgO–Al_2O_3–SiO_2–ZrO_2$ system, which exhibits efficient bulk nucleation, are investigated. In contrast to most published work on glasses in the $MgO–Al_2O_3–SiO_2$ system, clino-enstatite rather than cordierite is the major crystal phase to form in this case. The main objective of the present study was to gain an insight into the interaction between sintering and crystallization during the densification of this glass powder because it is a candidate matrix material for a range of ceramic matrix composites.

0022–2461

2. Experimental procedure

2.1. Material preparation

The glass composition was based on stoichiometric enstatite ($MgSiO_3$) with the addition of Al_2O_3 to aid glass stability and ZrO_2 as a nucleating agent. The glass was prepared by melting high-purity oxide ingredients at 1620 °C in an ODS (oxide dispersion strengthened) platinum crucible. The 1 kg melt was cast into cold water after 2 h at the melting temperature, and the resultant glass frit was crushed, dried and remelted at 1620 °C for a further 2 h to ensure good homogeneity. Most of the melt was then cast into cold water to provide frit for milling. Finally, a block of glass, approximately 30 mm × 60 mm × 15 mm was produced by casting the remainder of the melt into a pre-heated mild steel mould. This block was annealed at 750 °C for 1 h and allowed to cool slowly to room temperature; it was to be used in studies of the bulk crystallization processes.

The glass frit which had been produced by quenching the melt into cold water, was dried and subsequently dry milled with large alumina pebbles for 2 h, then sieved to yield a coarse powder of particle size $< 700\ \mu m$. This coarse powder was then wet milled in an aluminous porcelain mill jar with alumina pebbles. A 1.5 wt% aqueous solution of Dispex A40 (Allied Colloids Ltd., Bradford, UK) was used as the milling/suspending medium, with an appropriate amount being added to give a solids content of 70 wt% in the milling suspension. A total wet-milling time of 48 h was given, after which the average particle size was found to be 5–10 μm using a Malvern Instruments 3600D particle size analyser.

The milled glass powder suspension was decanted into a glass beaker and poured into rectangular polystyrene moulds which were placed on a Plaster of Paris base to form green bodies approximately 45 mm × 75 mm × 7 mm in size. These were dried for 2 days at room temperature before being used in the sintering trials. The green density of all the slip-cast bodies was later found to be 61% ± 1%.

2.2. Sintering trials

Samples for the sintering trials were obtained by carefully sawing the slip-cast bodies into strips approximately 45 mm × 10 mm × 7 mm in size. Each strip was sintered isothermally for a period of betwen 7.5 min and 100 h at a sintering temperature of between 800 and 840 °C. The linear shrinkage occurring during sintering was calculated from the initial and final length of each sample. Following sintering, the average thermal expansion coefficient over the temperature range 25–700 °C was measured and the data used in the crystallization studies. The thermal expansion measurements were performed on a horizontal axis, silica pushrod dilatometer, on samples approximately 3 mm × 4 mm × 40 mm, using a heating rate of 6 °C min^{-1}.

It was not possible to measure the density of many of the sintered samples directly as most of them contained a significant degree of open porosity. To enable the sintered density (and green density) to be determined, all samples were sintered to high density by a further heat-treatment at 1050 °C for 10 h. The samples had zero open porosity after this heat-treatment stage, and their densities were then readily determined using the Archimedes' method. The densities in the green state and after the sintering stage of heat-treatment were calculated from the final density and the initial, intermediate and final lengths of each sample, assuming that the shrinkage in these slip-cast powder compacts was isotropic.

2.3. Crystallization studies

During crystallization of the $MgO–Al_2O_3–SiO_2–ZrO_2$ glass under study there is a significant increase in linear thermal expansion coefficient from $65 \times 10^{-7}\ °C^{-1}$ for the glass to $100 \times 10^{-7}\ °C^{-1}$ for the fully heated material over the temperature range 25–700° C. Measurement of the thermal expansion coefficient, therefore, provided a convenient and semi-quantitative means of following the progress of the crystallization process. As mentioned in the previous section, thermal expansion measurements were performed on samples approximately 3 mm × 4 mm × 40 mm cut from the sintered strips.

In support of the thermal expansion measurements, scanning electron microscopy (SEM) was used to follow the crystallization process. The sintered samples were fractured and the fresh fracture surfaces etched for 20 s in 5% HF before being coated with a thin film of carbon and examined under the electron microscope. In addition to the electron microscopy, X-ray diffractometry (XRD) was used to provide information on the crystallization process.

As well as the increase in expansion coefficient of the material on heat-treatment, there is a considerable increase in bulk density (+ 11%) which has to be taken into account in the assessment of the densification behaviour. The increase in density which was due to crystallization was determined by performing heat-treatment trials on bulk-derived material. A number of specimens, approximately 3 mm × 4 mm × 40 mm, were cut from the cast and annealed block of glass and subjected to heat-treatments of between 0 and 32 h at 840 °C. Following heat-treatment, the density of each specimen and its thermal expansion coefficient (25–700 °C) were measured. This enabled a direct correlation between bulk density and thermal expansion coefficient to be drawn up, which, when used in conjunction with the thermal expansion data from the sintered specimens, permitted the shrinkage due to crystallization to be determined independently of the shrinkage due to sintering.

In allowing data derived from heat-treatment trials on bulk material to be applied in the interpretation of shrinkage data measured on power processed material, it is assumed that the types of crystal phase which develop, and the order in which they develop, are the same in each case (though the kinetics of the crystallization process need not be the same). This is considered to be justified because the evolution of expansion coefficient with heat-treatment temperature was similar in both cases, and the XRD spectra for the fully heat-treated materials were the same, irrespective of whether the glass-ceramic had been produced via

a powder or bulk route. The main reason for this apparent similarity in crystallization behaviour is thought to be the influence of the ZrO_2 as a homogeneous nucleation agent.

3. Results and discussion

3.1. Sintering behaviour

The linear shrinkage results are presented in Fig. 1, and the densification behaviour represented in Fig. 2. From these results it can be seen that the initial rate of shrinkage, $\dot{S}_0$, at any one temperature is almost linear, and that for every 10 °C temperature rise the initial linear shrinkage rate approximately doubles. Plotting $\ln(\dot{S}_0)$ against $1/T$ for the different sintering temperatures yields an apparent activation energy for this initial stage of sintering of 615 ± 40 kJ mol^{-1}. This is similar to the activation energy for sintering of a crystallizable CaO–Al_2O_3–ZnO–SiO_2-based glass studied by Clark and Reed [8].

After a certain time at the sintering temperature the thermal expansion coefficient of the sintered material starts to increase, signifying that crystal phases are being developed (Fig. 3). Because the crystallization process is accompanied by a significant increase in density, any crystallization occurring during sintering will distort the densification data. To follow the sintering process it is necessary to take account of any shrinkage due to crystallization. To arrive at the shrinkage due to crystallization, the expansion coefficient of the sintered specimens was measured to establish the degree of crystallization. The studies on the bulk-derived materials were then used to relate the degree of crystallization to the bulk density via the thermal expansion coefficient. Fig. 4 shows the relationship between the expansion coefficient and the density of the bulk-derived material as the degree of crystal phase development increases.

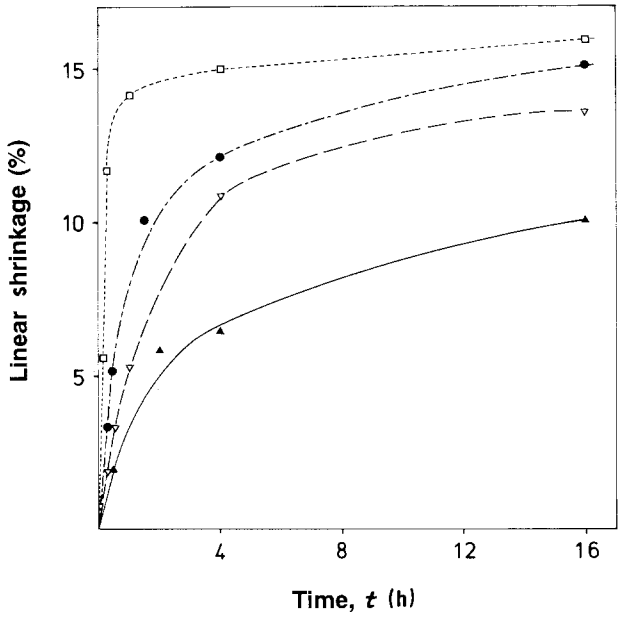

Figure 1 Graph showing linear shrinkage of glass powder compacts versus time, for sintering temperatures of (▲) 800 °C, (▽) 810 °C, (●) 820 °C and (□) 840 °C.

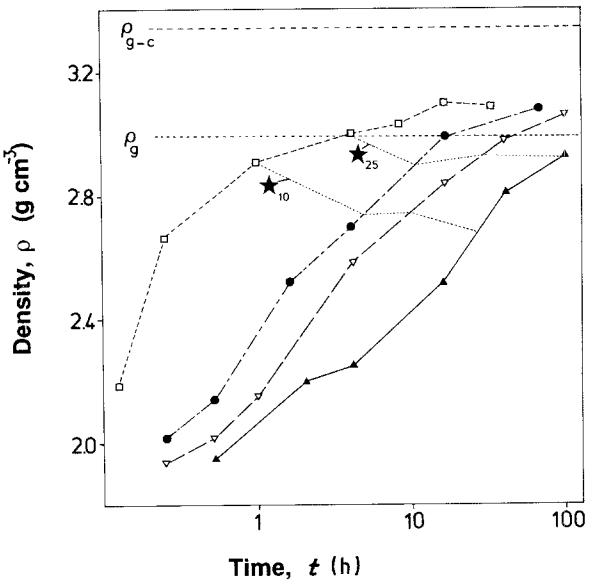

Figure 2 Variation of density versus time for glass powder samples sintered at (▲) 800 °C, (▽) 810 °C, (●) 820 °C and (□) 840 °C. ρ_g and ρ_{g-c} indicate densities of annealed glass and fully heat-treated glass-ceramic, respectively. ($\bigstar_{10}$, $\bigstar_{25}$) Degrees of crystallization of 10% and 25%, respectively.

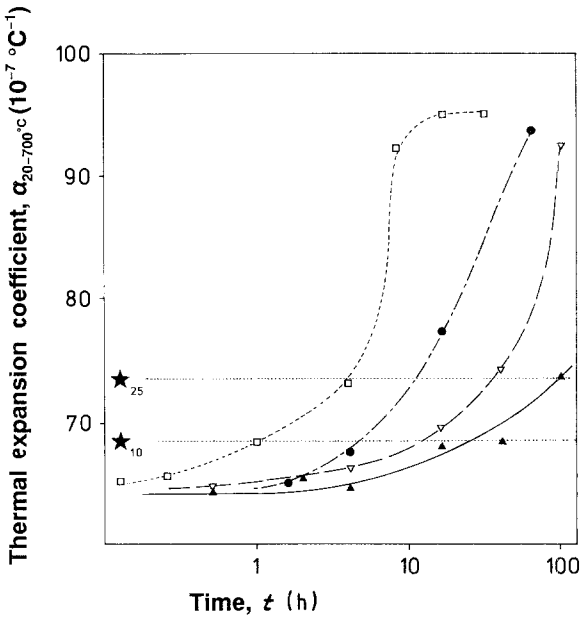

Figure 3 Increase of linear thermal expansion coefficient with time for glass powder samples sintered at (▲) 800 °C, (▽) 810 °C, (●) 820 °C and (□) 840 °C. ($\bigstar_{10}$, $\bigstar_{25}$) α values corresponding to 10% and 25% degrees of crystallization, respectively.

The densification results, corrected for increases in density due to crystallization, are shown in Fig. 5. The results are presented as a relative density (density of sintered compact divided by the density of the bulk material with the same degree of crystallization), to enable the sintering process to be followed more readily, and to show clearly how the degree of porosity varies with sintering time and temperature. It is apparent from Fig. 5 that relative densities of 95%–98% can be achieved during the sintering process at the various temperatures employed, and that at more extended sintering times there is a slight but important decrease

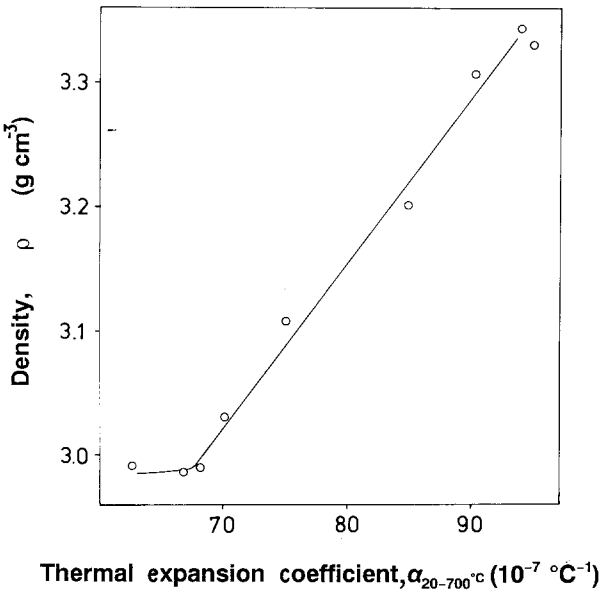

Figure 4 Relationship between density and expansion coefficient for bulk processed glass, heat-treated for various times at 840 °C.

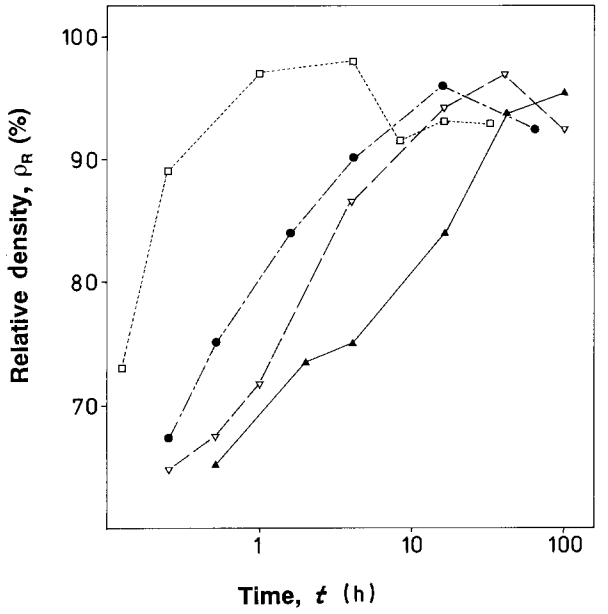

Figure 5 Variation of relative density versus time for glass powder samples sintered at (▲) 800 °C, (▽) 810 °C, (●) 820 °C and (□) 840 °C.

in relative density. The possible reasons for this are discussed later.

3.2. Crystallization behaviour

Analysis of the thermal expansion results on the sintered bodies (Fig. 3) reveals that both the onset of crystallization and the rate of crystallization are more rapid at the higher sintering temperatures. By defining the degree of crystallization as

$$C(\%) = (\alpha - \alpha_{glass})/(\alpha_{glass\text{-}ceramic} - \alpha_{glass}) \quad (1)$$

it is possible to quantify the extent of crystallization as it evolves through the sintering process. The time taken to reach a degree of crystallization of 10% and 25% ($\alpha = 68.5 \times 10^{-7}$ and 74×10^{-7} °C^{-1}, respectively) at each of the sintering temperatures was determined from Fig. 3. These times are plotted on Fig. 2 across the densification curves to indicate at which stage in the densification process these degrees of crystallization had been reached.

Examination of Fig. 2 shows that the initial rate of sintering relative to the rate of crystallization is significantly higher at 840 °C than in the temperature range 800–820 °C. In considering the kinetics of the sintering and crystallization processes it should be borne in mind that for homogeneously nucleated materials there is generally an incubation period for the formation of stable crystal nuclei [11]. Because the sintering process is not subject to such an incubation period, some degree of sintering would be expected to occur before crystallization starts in these materials.

The existence of an incubation period for homogeneous nucleus formation implies that crystallization could be avoided if a sufficiently high heating rate were employed. Whilst this may be valid for bulk-processed materials, it is unlikely to be so in powder-processed materials because there is a population of heterogeneous (surface) nucleation sites which should be active from the initial stages of any sintering process. Thus, to obtain high densities in sintered glass-ceramics it is often necessary to suppress surface-nucleated crystallization by selecting relatively coarse glass powders, or removing surface nucleation sites by chemical treatment of the starting powders [8, 10].

The observation in this study that crystallization is delayed until further into the sintering process at 840 °C suggests that, relative to the speed of sintering, the incubation period for the development of effective nucleation sites for crystal growth is longer than at the lower sintering temperatures. Although the onset of crystallization appears to be delayed at the highest sintering temperature, the differences in the relative progress of the sintering and crystallization processes become much less pronounced over the range of sintering temperatures used as the degree of crystallization increases. If Figs 2 and 5 are compared, it can be seen that the point at which maximum relative density has been reached corresponds to a degree of crystallization of approximately 25% in all cases. The measured data indicate that a slightly higher peak relative density is reached in the material sintered at 840 °C than in those sintered in the temperature range 800–820 °C. This may be a consequence of the initially higher ratio of sintering rate to crystallization rate observed at 840 °C. However, the apparent differences in the relative density maxima are small, and it is not clear whether they are real, or a consequence of the positioning of experimental data points on the sintering curve. It is clear, however, that at each of the sintering temperatures, it is possible to achieve a high relative density at a stage where there is a significant degree of crystal phase development, proving that it is not always necessary to delay the start of crystallization until sintering is complete in order to achieve a high-density material.

To establish an approximate activation energy for crystallization, the initial crystallization rate, $\dot{C}_0$, was estimated from the time taken to reach a

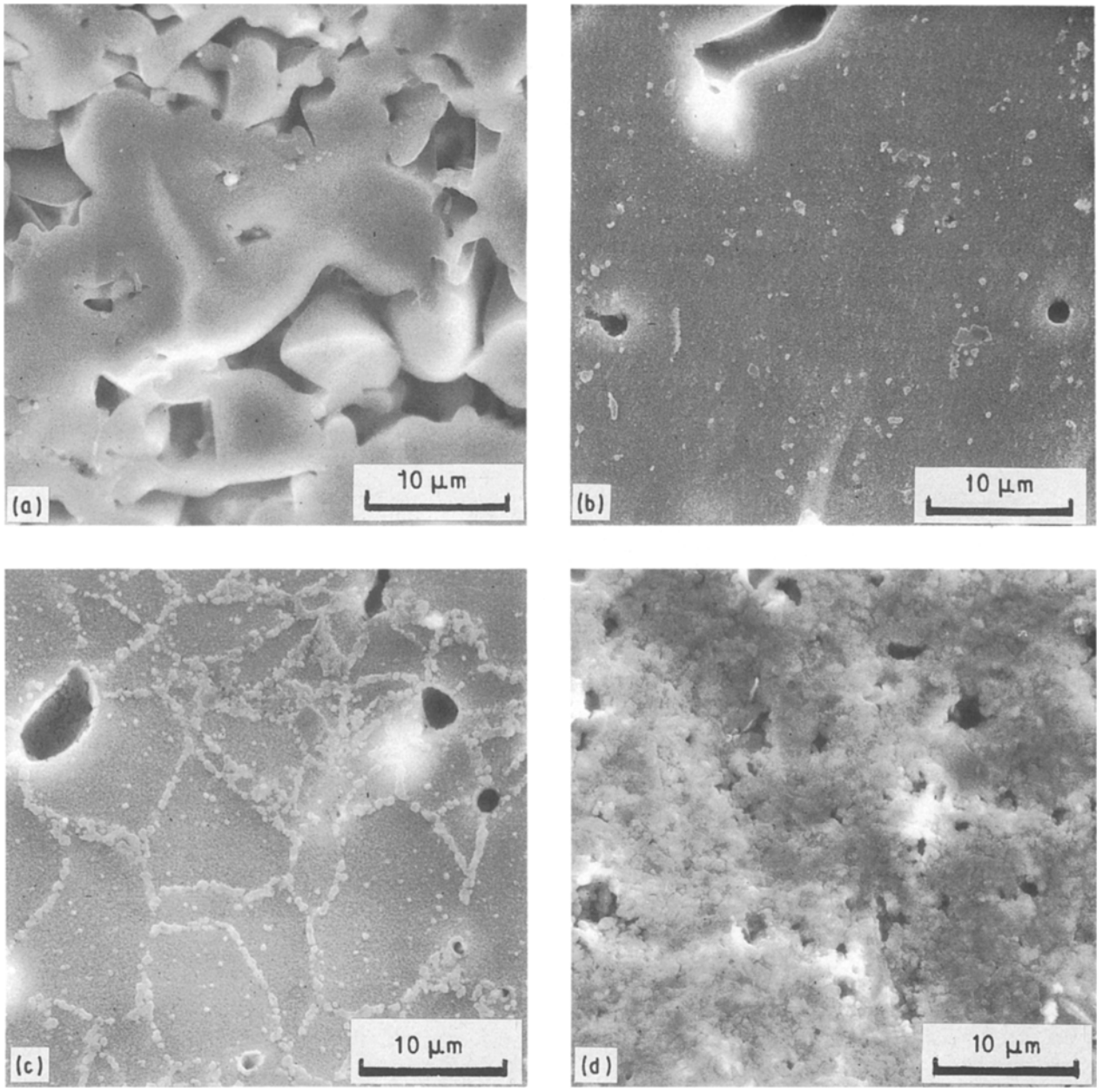

Figure 6 Scanning electron micrographs of etched fracture surfaces of powder compacts sintered at 840 °C for (a) 15 min, (b) 1 h, (c) 4 h and (d) 8 h.

degree of crystallization of 10%. Plotting $\ln(\dot{C}_0)$ against $1/T$ gives an apparent activation energy of 820 ± 50 kJ mol^{-1}. Although this figure seems reasonable, it should only be regarded as an estimate because, in its derivation, no account was taken of the influence of the expected incubation period for homogeneous nucleus formation, or possible differences in nucleation density at the different sintering temperatures.

The SEM observations on etched fracture surfaces of partially and fully sintered powder compacts provide a good insight into the processes occurring during densification. Fig. 6 shows electron micrographs of material sintered at 840 °C for periods of between 15 min and 8 h. By comparing Fig. 6a and b it can be seen that almost all of the fine-scale porosity is eliminated within 1 h at 840 °C; and at this stage the larger pores which remain account for nearly all of the porosity (which by reference to Fig. 5 is approximately 3%). After 4 h at 840 °C (Fig. 6c) there is clear evidence of crystallization which appears to have nucleated at the former surfaces of the original glass powder particles, following their deformation during sintering. A number of crystals which have been nucleated within the original glass particles are also visible.

Examination of these etched, fracture surfaces at high magnification (Fig. 7) shows that there is a dispersion of very fine particles, 50–100 nm diameter, throughout the entire material. This dispersion of fine particles, identified as cubic zirconia (c-ZrO_2) by XRD, is already present after 1 h at 840 °C and could be expected to nucleate crystallization of secondary phases. After 4 h at 840 °C (Fig. 7b), there is some evidence that these fine particles have either coarsened somewhat, or have encouraged the crystallization of further crystal phases.

One striking feature is that the former particle surfaces are the sites where crystal growth is most advanced, even though after 1 h at 840 °C there is no

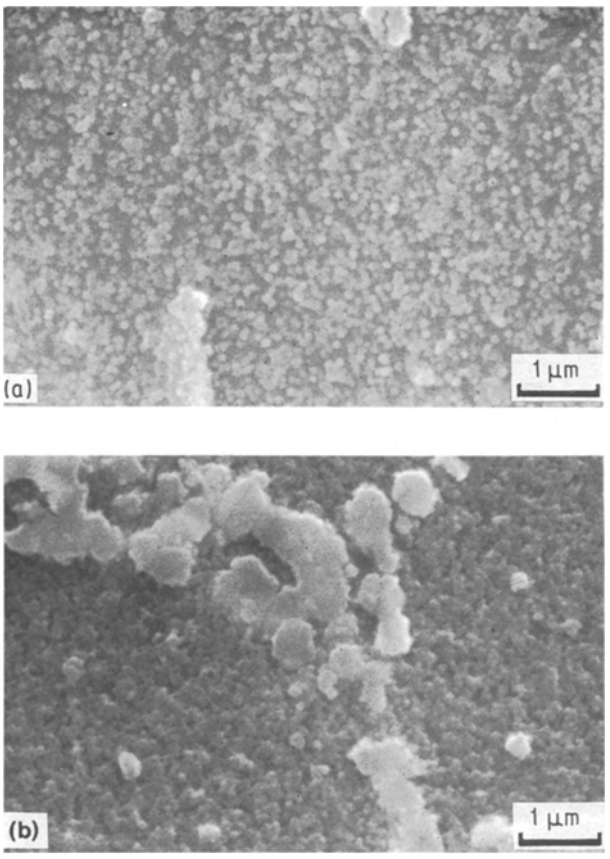

Figure 7 Scanning electron micrographs of etched fracture surfaces of powder compacts heat-treated at 840 °C for (a) 1 h and (b) 4 h.

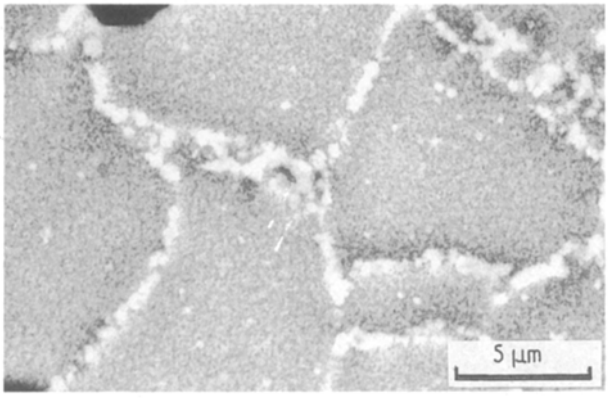

Figure 8 Back-scattered electron image of an etched fracture face of a powder compact heat-treated at 840 °C for 1 h. ZrO_2 segregation at the former particle surfaces is apparent, and some zones of ZrO_2 depletion are visible adjacent to the former particle surfaces.

microstructural evidence that these surfaces are present. In Fig. 8, showing a back-scattered electron image of the material heat-treated for 4 h at 840 °C, there appears to be some segregation of zirconia at the former particle surfaces which may explain the locally enhanced crystallization. There is also the suggestion that some zones adjacent to these ZrO_2-rich regions have a lower population of the fine c-ZrO_2 precipitates. These zones of apparent ZrO_2 depletion, however, are not situated symmetrically about the ZrO_2-rich regions. One possible explanation for this is that the fine c-ZrO_2 precipitates form early in the sintering process and, having a mobility which is different from that of the residual glassy phase, tend to segregate as the glass-particle boundaries migrate to eliminate porosity during sintering. The fact that the fine c-ZrO_2 precipitates form early in the sintering process is demonstrated by the results of the XRD analyses.

It is clear from Fig. 9, showing how the crystal phases develop during sintering at 800 °C, that a detectable amount of c-ZrO_2 develops as early as 2 h into the sintering process at this temperature, a stage where the relative density is less than 75%. It appears that the precipitation of the fine c-ZrO_2 particles is almost complete after 16 h at 800 °C, whereas the maximum relative density of $\sim 95\%$ is not attained until about 100 h at this temperature. This shows that much of the sintering takes place after the c-ZrO_2 has precipitated, so segregation due to the different mobilities of the ZrO_2 precipitates and the residual glassy phase certainly seems possible. The next crystal phase to develop following the precipitation of the c-ZrO_2 has been identified as clino-enstatite ($MgSiO_3$) by XRD. This is clearly present after 100 h at 800 °C (Fig. 9) and is the major crystal phase present in the material after the full heat-treatment of 1050 °C for 10 h.

After 8 h at 840 °C, the crystallization sequence appears to be almost complete, and once again there is no visible evidence of the original glass-particle surfaces. The uniformity of the microstructure suggests that bulk-nucleated crystallization occurs sufficiently

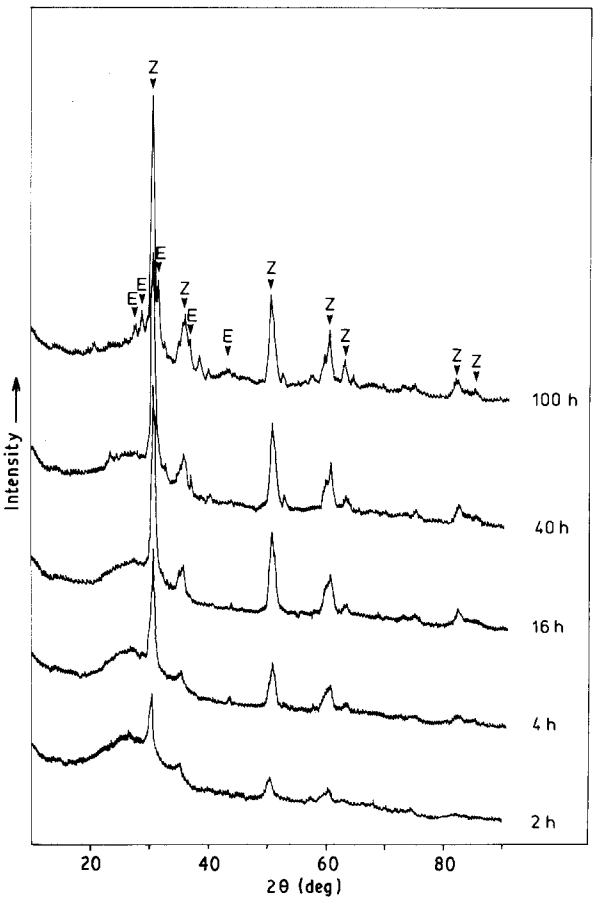

Figure 9 XRD traces showing development of crystal phases in powder compacts heat-treated at 800 °C for periods of between 2 and 100 h. Z = c–ZrO_2 and E = $MgSiO_3$ (clino-enstatite).

rapidly to prevent the crystals which are nucleated at the former particle surfaces becoming over-enlarged.

Fig. 5 shows that as the crystallization proceeds to completion at 840 °C, the relative density decreases significantly, from approximately 98% to less than 92%. Comparison of Figs 6c and d shows how the pore morphology and distribution change as the glass-ceramic crystallizes. The crystallization is accompanied by an increase in density of about 11%, and as it proceeds, material appears to be drawn back from the pore surfaces to accommodate the necessary material shrinkage. The pore surfaces lose their smooth contours as the material crystallizes, and some new, small, irregular pores are seen to open up in the bulk of the material.

The crystallization and densification data suggest that the shrinkage due to crystallization can be accommodated by the material in the initial stages of crystallization without the development of porosity; presumably by flow of the residual glass phase. Once the degree of crystallization exceeds a certain limit, though, it appears that the developing crystallites form a rigid skeleton so that further shrinkage due to crystallization cannot be accommodated by long-range deformation of the material. Instead, it seems that the shrinkage is taken up locally by the enlargement of existing pores or the opening up of new ones once the degree of crystallization, as defined earlier, exceeds about 25%.

This is in contrast to the behaviour of the bulk-processed material, which although undergoing a similar crystallization sequence, remains fully dense throughout the whole process. It is believed that this is due to the difficulty of pore nucleation in the bulk-processed material. It is not clear whether a powder-processed material would remain fully dense throughout the crystallization process if the porosity had previously been totally eliminated during sintering.

Although the crystallization behaviour of the bulk and powder derived materials is similar in many respects, i.e. precipitation of very fine c-ZrO_2 particles, followed by development of clino-enstatite as the major crystal phase, there are at least two differences which could account for the fact that the relative density of the powder-processed material decreases during crystallization whereas that of the bulk-derived material does not. The first difference is the accelerated development of crystallites at the former glass-particle boundaries in the powder-processed material, which may lead to the premature formation of a rigid skeleton in the material which prevents long-range deformation, and forces the shrinkage due to further crystallization to be accommodated internally by the development of porosity.

Another aspect, which may influence the opening up of porosity in the powder-processed material, is the presence of gases in the pores, as these materials were sintered in air. At some stage during the sintering process the pores lose their interconnectivity, so any gases which are present can no longer escape. As these closed pores shrink during sintering, the gas pressure within the pores increases, with the result that further pore shrinkage might be inhibited. In the material under investigation in this study, much of the fine porosity is eliminated during sintering, suggesting that the gas which was originally trapped within these pores dissolves into the surrounding glass-ceramic material, which at this stage is predominantly glassy. The elimination of the fine-scale porosity in preference to the coarser pores is thought to be due to the higher surface area to volume ratio of the fine pores which will aid in gas dissolution.

Towards the end of the sintering process, then, a few large pores containing gas are present in a matrix which has a very fine dispersion of c-ZrO_2 precipitates and some clino-enstatite crystallites developing at the former glass-particle surfaces. The level of dissolved gas in the matrix is also high owing to the prior elimination of fine gas-filled pores from the material. This enhanced level of dissolved gas in the powder-processed material is likely to encourage the enlargement of existing pores and the nucleation of new pores as the material shrinks during crystallization, especially if the solubility of the dissolved gas is much lower in the crystalline phases than in the initial glassy phase. Low pressure or vacuum sintering may be useful as a means of limiting the amount of gas dissolving in the material, and may help reduce pore generation/enlargement during crystallization.

Pore enlargement has been reported in other powder-processed glass-ceramic systems during the later stages of heat-treatment. The increase in porosity was attributed to the volume change on crystallization of a CaO–MgO–Al_2O_3–SiO_2 based glass-ceramic studied by Kim *et al.* [6], whereas Mussler and Shafer [10] ascribed the pore enlargement and agglomeration in a cordierite + ZrO_2-based glass-ceramic at temperatures of $> 1000\,°C$ to H_2O and CO_2 desorption. In the present study, it is believed to be a combination of the large volume change on crystallization and the release of dissolved gases which is responsible for the increase in porosity.

For the material heat-treated at 840 °C for periods in excess of 8 h, there is a small, but significant increase in the relative density from 91.5% to 93% showing that some densification is possible even with a high volume fraction of crystalline phases present.

All materials were given a second heat-treatment stage of 1050 °C for 10 h after their initial sintering heat-treatment stage in the temperature range 800–840 °C in order to complete the crystallization process. Irrespective of the degree of densification attained during the sintering stage at 800–840 °C, all materials reached a relative density at the end of the second heat-treatment stage of 94% ± 1%. This suggests that the densification process in this material is rather insensitive to variations in the heat-treatment schedule, so long as the final temperature is high enough to allow crystallization to be completed. Supporting this finding, it has been observed that on heating a slip-cast body of the glass powder directly to the 10 h hold at 1050 °C at a rate of $5\,°C\,min^{-1}$, the relative density is also 94% ± 1%. In all cases, the majority of the porosity present in the fully heat-treated material appears to be a result of the volume

shrinkage and possible gas release on crystallization, and not due to insufficient densification during sintering.

4. Conclusion

It has been demonstrated that a clino-enstatite-based glass-ceramic can be produced by the sintering and crystallization of a suitable glass powder in the $MgO–Al_2O_3–SiO_2–ZrO_2$ system.

At an early stage of the sintering process, a very fine dispersion of c-ZrO_2 precipitates, 50–100 nm diameter, is observed, but this appears not to inhibit further sintering of the glass powder. From measurements of the temperature dependence of the linear shrinkage rate during the initial stages of sintering, an apparent activation energy for sintering of $615 \pm 40\ kJ\ mol^{-1}$ has been calculated. At some stage before peak relative density is reached, clino-enstatite is observed to start crystallizing from the glassy phase, with the rate of crystallization enhanced at the former surfaces of the glass particles. The rate of homogeneously nucleated crystallization within the glass particles, however, is sufficient to prevent the excessive enlargement of the clino-enstatite grains which have been nucleated at the former glass-particle boundaries, so a fine, uniform microstructure is produced. A substantial degree of crystallization ($\sim 25\%$) appears to be reached by the time the maximum relative density of 95%–98% is achieved, proving that efficient sintering is possible in the presence of developing crystal phases.

As the degree of crystallization increases above $\sim 25\%$, the material is no longer able to accommodate the volume change which accompanies crystallization by long-range deformation/shrinkage. Instead, the crystallization shrinkage is accommodated locally by the enlargement of already existing pores or the opening up of new ones; a process which is thought to be aided by the release of dissolved gases from the glass-ceramic as it crystallizes. By the time the crystallization process is complete, the opening up of the porosity causes the relative density to decrease to $\sim 92\%$. Heat-treatment to higher temperatures causes some further densification, but in no case is the final relative density found to exceed 95%. As long as the heat-treatment schedule is sufficient to cause complete crystallization, the final density appears to have very little dependence on the heating rates or holding temperatures used in the thermal processing.

References

1. H. T. SAWHILL, R. H. JENSON and K. R. MIKESKA, in "Proceedings of the Symposium on Materials and Processes for Microelectronic Systems", Anaheim, CA, 31 October-3 November 1989, Ceramic Transactions Vol. 15 (American Ceramic Society, 1990) pp. 611–28.
2. G. PARTRIDGE, C. A. ELYARD and A. K. DATTA, "Fabrication of glass-ceramics by tape casting", in British Ceramic Proceedings no. 45, "Fabrication Technology" (The Institute of Ceramics, Stoke-on-Trent, UK, 1990) pp. 123–9.
3. E. M. RABINOVICH, "Cordierite glass-ceramics produced by sintering", Advances in Ceramics Vol. 4, "Nucleation and Crystallization in Glasses", edited by J. H. Simmons, D. R. Uhlmann and G. H. Beall (American Ceramic Society, Columbus, Ohio, 1982) pp. 327–33.
4. M. N. RAHAMAN, in "Proceedings of the International Symposium on Advances in Processing of Ceramic and Metal Matrix Composites", Halifax Nova Scotia, Canada, 20–24 August 1989, pp. 71–79.
5. V. S. R. MURTHY and M. H. LEWIS, *Brit. Ceramic Trans. J.* **89**(5) (1990) 173.
6. H. S. KIM, R. D. RAWLINGS and P. S. ROGERS, *J. Mater. Sci.* **24** (1989) 1025.
7. A. R. HYDE and G. PARTRIDGE, "Fabrication of particulate, platelet, whisker and continuous fibre reinforced glass, glass-ceramic and ceramic materials", in British Ceramic Proceedings no. 45, "Fabrication Technology" (The Institute of Ceramics, Stoke-on-Trent, UK, 1990) pp. 221–27.
8. T. J. CLARK and J. S. REED, *J. Amer. Ceram. Soc.* **69** (1986) 837.
9. P. C. PANDA and R. RAJ, *ibid.* **72** (1989) 1564.
10. B. H. MUSSLER and M. W. SHAFER, *Amer. Ceram. Soc. Bull.* **64** (1985) 1459.
11. P. W. McMILLAN, "Glass-ceramics" (Academic Press, London, 1979) p. 32.

Received 28 October 1991
and accepted 17 February 1992